RIGID-ROTOR VLASOV EQUILIBRIUM FOR AN INTENSE CHARGED-PARTICLE BEAM PROPAGATING THROUGH A PERIODIC SOLENOIDAL MAGNETIC FIELD

Chiping Chen and Renato Pakter
Plasma Science and Fusion Center
Massachusetts Institute of Technology
Cambridge, Massachusetts 02139

Ronald C. Davidson
Plasma Physics Laboratory
Princeton University
Princeton, New Jersey 08543

ABSTRACT

A new rigid-rotor Vlasov equilibrium is obtained for an intense, axisymmetric charged-particle beam with uniform density in the radial direction propagating through a periodic solenoidal focusing field. The beam envelope equation is derived, and examples of periodically focused rigid-rotor Vlasov equilibria are presented. Statistical properties and possible applications of the present beam equilibrium are also discussed.

PACS Numbers: 29.27.-a, 41.75.-i, 41.85.-p

A fundamental understanding of the kinetic equilibrium and stability properties of an intense charged-particle beam in periodic electric and magnetic fields is important to the development of advanced particle accelerators and advanced coherent radiation sources for a wide range of applications [1-3]. Until this paper, the Kapchinskij-Vladimirskij (KV) equilibrium [4] has been the only known collisionless (Vlasov) equilibrium for continuous intense charged-particle beams propagating through either an alternating-gradient quadrupole magnetic focusing field [4,5] or a periodic solenoidal focusing field [5,6]. Studies of the KV beam equilibrium and its stability properties [1-7] have contributed significantly to the physics of intense charged-particle beams.

A large body of literature exists on the Vlasov equilibrium and stability properties of rotating nonneutral charged-particle beams propagating parallel to a *uniform* solenoidal focusing field $B_0\vec{e}_z$ [8], where $B_0 =$ const., dating back to the original work of Davidson and Krall [9]. In the present paper, it is shown that there exists a rigid-rotor Vlasov equilibrium for an intense charged-particle beam with uniform density in the radial direction propagating through a *periodic* solenoidal focusing field. In the present analysis, the beam is assumed to have a uniform density profile in the radial direction, and a rigid-rotor angular flow velocity in addition to a constant axial velocity $\beta_b c$. As special limiting cases, the present analysis includes both the familiar KV equilibrium for an intense beam propagating through a periodic solenoidal focusing field [6,8], and the familiar uniform-density rigid-rotor Vlasov equilibrium in a uniform solenoidal field [10]. The beam envelope equation is derived and used to determine the axial dependence of the outer beam radius. Statistical properties and possible applications of the present beam equilibrium are also discussed.

We consider a thin, continuous, axisymmetric $(\partial / \partial\theta = 0)$, intense charged-particle beam propagating with constant axial velocity $\beta_b c\vec{e}_z$ through an applied periodic solenoidal focusing field. The applied solenoidal focusing field inside the thin beam can be approximated by

$$\vec{B}^{ext}(r,s) = B_z(s)\vec{e}_z - \frac{r}{2}B_z'(s)\vec{e}_r, \tag{1}$$

where $s = z$ is the axial coordinate, $r = \left(x^2 + y^2\right)^{1/2}$ is the radial distance from the beam

axis, $B_z(s+S) = B_z(s)$ is the axial magnetic field, S is the fundamental periodicity length of the focusing field, and prime denotes derivative with respect to s. Here, $S >> r_b$ is assumed, where r_b is the characteristic radius of the outer beam envelope. To determine the self-electric and self-magnetic fields of the beam self-consistently, we assume that the density profile of the beam is uniform, i.e.,

$$n_b(r,s) = \begin{cases} N / \pi r_b^2(s), & 0 \le r < r_b(s), \\ 0, & r > r_b(s), \end{cases} \tag{2}$$

where $r_b(s) = r_b(s+S)$ is the equilibrium beam radius, and $N = 2\pi \int_0^\infty dr r n_b(r,s) =$ const. is the number of particles per unit axial length. In the paraxial approximation, the Budker parameter of the beam is assumed to be small compared with unity, i.e., $q^2 N / mc^2 << 1$, and the transverse kinetic energy of a beam particle is assumed to be small compared with its axial kinetic energy. Here, c is the speed of light in *vacuo*, and q and m are the particle charge and rest mass, respectively. From the equilibrium Maxwell equations, we find that the self-electric and self-magnetic fields, $E_r^s \vec{e}_r$ and $B_\theta^s \vec{e}_\theta$, are given by

$$E_r^s(r,s) = \beta_b^{-1} B_\theta^s(r,s) = \frac{2qNr}{r_b^2(s)} \tag{3}$$

in the beam interior $\left(0 \le r < r_b\right)$. It is convenient to express the self fields in terms of the scalar and vector potentials defined for $0 \le r < r_b(s)$ by

$$\Phi^s(r,s) = \beta_b^{-1} A_z^s(r,s) = -\frac{qNr^2}{r_b^2(s)}, \tag{4}$$

where $\vec{A}^s(r,s) = A_z^s(r,s)\vec{e}_z$, $E_r^s(r,s) = -\partial \Phi^s / \partial r$, and $B_\theta^s(r,s) = -\partial A_z^s / \partial r$. Furthermore, we choose the vector potential for the applied periodic solenoidal field to be $\vec{A}^{ext}(r,s) = (r/2) B_z(s) \vec{e}_\theta$ with $\vec{B}^{ext}(r,s) = \nabla \times \vec{A}^{ext}(r,s)$.

It can be shown that the transverse motion for an individual particle in the combined fields, $\vec{B}^{ext}(r,s) + B_\theta^s(r,s)\vec{e}_\theta$ and $E_r^s(r,s)\vec{e}_r$, are described by the normalized perpendicular Hamiltonian $\hat{H}_\perp = H_\perp / \gamma_b \beta_b^2 mc^2$ [6]

$$\hat{H}_{\perp}\left(x,y,\hat{P}_x,\hat{P}_y,s\right)=\frac{1}{2}\left\{\left[\hat{P}_x+y\sqrt{\kappa_z(s)}\right]^2+\left[\hat{P}_y-x\sqrt{\kappa_z(s)}\right]^2-\frac{K}{r_b^2(s)}\left(x^2+y^2\right)\right\}. \quad (5)$$

Here, $\left(x,\hat{P}_x\right)$ and $\left(y,\hat{P}_y\right)$ are canonical conjugate pairs, $\sqrt{\kappa_z(s)}=qB_z(s)/2\gamma_b\beta_b mc^2$ is the normalized Larmor frequency, $K=2q^2N/\gamma_b^3\beta_b^2mc^2$ is the self-field perveance [1], $\gamma_b=\left(1-\beta_b^2\right)^{-1/2}$ is the relativistic mass factor, and the normalized transverse canonical momentum $\hat{\vec{P}}_{\perp}=\left(\hat{P}_x,\hat{P}_y\right)$ is related to the transverse mechanical momentum $\vec{p}_{\perp}$ by $\hat{\vec{P}}_{\perp}=\left(\gamma_b\beta_b mc\right)^{-1}\left(\vec{p}_{\perp}+q\vec{A}_{\perp}^{ext}/c\right)$. It is useful to introduce the canonical transformation from the Cartesian canonical variables $\left(x,y,\hat{P}_x,\hat{P}_y\right)$ to the new canonical variables $\left(X,Y,P_X,P_Y\right)$ in the Larmor frame defined by [6]

$$\begin{aligned}
x&=wX\cos\phi+wY\sin\phi,\\
y&=-wX\sin\phi+wY\cos\phi,\\
\hat{P}_x&=\left(w^{-1}P_X+w'X\right)\cos\phi+\left(w^{-1}P_Y+w'Y\right)\sin\phi,\\
\hat{P}_y&=-\left(w^{-1}P_X+w'X\right)\sin\phi+\left(w^{-1}P_Y+w'Y\right)\cos\phi.
\end{aligned} \quad (6)$$

In Eq. (6), $\phi(s)=\int_{s_0}^{s}ds\sqrt{\kappa_z(s)}$ is the accumulated phase of rotation of the Larmor frame of reference relative to the laboratory frame, the periodic function $w(s)=w(s+S)$ solves the differential equation

$$w''(s)+\left[\kappa_z(s)-\frac{K}{r_b^2(s)}\right]w(s)=\frac{1}{w^3(s)}, \quad (7)$$

and prime denotes derivative with respect to s. The canonical transformation in Eq. (6) can be obtained by successive applications of the generating functions

$$F_2\left(x,y;\tilde{P}_x,\tilde{P}_y,s\right)=\left(x\cos\phi-y\sin\phi\right)\tilde{P}_x+\left(x\sin\phi+y\cos\phi\right)\tilde{P}_y, \quad (8)$$

$$\tilde{F}_2\left(\tilde{x},\tilde{y};P_X,P_Y,s\right)=\left(\tilde{x}P_X+\tilde{y}P_Y\right)/w+\left(w'/2w\right)\left(\tilde{x}^2+\tilde{y}^2\right). \quad (9)$$

It follows from Eq. (8) that $\tilde{x}=x\cos\phi-y\sin\phi$ and $\tilde{y}=x\sin\phi+y\cos\phi$. The Hamilton equations for the perpendicular motion in the Larmor frame can be expressed as

$$\vec{X}' = \frac{\partial H}{\partial \vec{P}} = \frac{\vec{P}}{w^2(s)},$$
$$\vec{P}' = -\frac{\partial H}{\partial \vec{X}} = -\frac{\vec{X}}{w^2(s)}, \tag{10}$$

where $\vec{X} = (X, Y)$, $\vec{P} = (P_X, P_Y)$, and the new Hamiltonian is defined by

$$H(X, Y, P_X, P_Y, s) = \frac{1}{2w^2(s)}\left(X^2 + Y^2 + P_X^2 + P_Y^2\right). \tag{11}$$

Because $A_X^2 = X^2 + P_X^2$, $A_Y^2 = Y^2 + P_Y^2$, and the canonical angular momentum $P_\Theta = XP_Y - YP_X$ are *exact* single-particle constants of the motion for the Hamiltonian in Eq. (5), we define a possible choice of Vlasov equilibrium distribution function by

$$f_b(X, Y, P_X, P_Y) = \frac{N}{\pi^2 \varepsilon_T}\delta\left[X^2 + Y^2 + P_X^2 + P_Y^2 - 2\omega_b\left(XP_Y - YP_X\right) - \left(1 - \omega_b^2\right)\varepsilon_T\right], \tag{12}$$

where $df_b / ds = 0 = \partial f_b / \partial s$, ε_T = const. > 0 is an effective emittance, $\delta(x)$ is the Dirac δ-function, and the rotation parameter ω_b = const. is allowed to be in the range $-1 < \omega_b < 1$ for radially confined equilibria. As shown below, Eq. (12) is consistent with the assumed density profile in Eq. (2). While f_b is defined in terms of a δ-function, it should provide a very good description of a well-matched beam equilibrium in experimental applications.

It is readily shown that the beam equilibrium described by the distribution function f_b in Eq. (12) has the following statistical properties. First, the beam has the uniform-density profile $n_b(r,s) = w^{-2}(s)\int f_b dP_X dP_Y$ prescribed by Eq. (2), provided $r_b(s) = \varepsilon_T^{1/2} w(s)$. In other words, the outer equilibrium radius of the beam $r_b(s) = r_b(s + S)$ obeys the familiar envelope equation [1,6]

$$\frac{d^2}{ds^2} r_b(s) + \kappa_z(s) r_b(s) - \frac{K}{r_b(s)} - \frac{\varepsilon_T^2}{r_b^3(s)} = 0. \tag{13}$$

Second, in dimensional units, the average (macroscopic) transverse velocity of the beam equilibrium described by Eq. (12) is given in the Larmor frame by

$$\tilde{\vec{V}}_\perp(r,s) = \left[n_b(r,s) w^2(s)\right]^{-1} \int \tilde{\vec{v}}_\perp f_b dP_X dP_Y = \frac{r_b'(s)}{r_b(s)} \beta_b c r \tilde{\vec{e}}_r + \tilde{\Omega}_b(s) r \tilde{\vec{e}}_\theta, \tag{14}$$

where $\tilde{\Omega}_b(s) = \tilde{V}_\theta(r,s)/r = \varepsilon_T \omega_b \beta_b c / r_b^2(s)$. Note in Eq. (14) that the azimuthal flow velocity $\tilde{V}_\theta(r,s)$ is proportional to the average (normalized) canonical angular momentum in the Larmor frame, $\langle \hat{P}_\theta \rangle(r,s) = [n_b(r,s) w^2(s)]^{-1} \int P_\Theta f_b dP_X dP_Y = \varepsilon_T \omega_b r^2 / r_b^2(s)$. In the laboratory frame, the s-dependent average transverse flow velocity and angular rotation velocity of the beam equilibrium described by Eq. (12) can be expressed as

$$\vec{V}_\perp(r,s) = [n_b(r,s) w^2(s)]^{-1} \int \vec{v}_\perp f_b dP_X dP_Y = \frac{r_b'(s)}{r_b(s)} \beta_b c r \vec{e}_r + \Omega_b(s) r \vec{e}_\theta, \tag{15}$$

$$\Omega_b(s) = \frac{\varepsilon_T \beta_b c}{r_b^2(s)} \omega_b - \frac{qB_z(s)}{2\gamma_b mc}, \tag{16}$$

respectively. Because the beam rotates macroscopically as a rigid body at a rate that is a periodic function of the axial propagation distance s, we refer to the Vlasov equilibrium described by Eq. (12) as a *periodically focused rigid-rotor Vlasov equilibrium*. As a third statistical property, the beam equilibrium described by Eq. (12) has the effective transverse temperature profile (in dimensional units)

$$T_\perp(r,s) = [n_b(r,s) w^2(s)]^{-1} \int \frac{\gamma_b m}{2} \left(\vec{v}_\perp - \vec{V}_\perp\right)^2 f_b dP_X dP_Y = T_\perp(0,s) \left[1 - \frac{r^2}{r_b^2(s)}\right], \tag{17}$$

where

$$T_\perp(0,s) = \left(1 - \omega_b^2\right) \frac{m\gamma_b \beta_b^2 c^2 \varepsilon_T^2}{2 r_b^2(s)}. \tag{18}$$

Note from Eq. (18) that the product $T_\perp(0,s) r_b^2(s)$ is a conserved quantity $(d/ds = 0)$ as the beam is axially modulated. As a fourth property, the *rms* emittance of the beam equilibrium described by Eq. (12) is given in the Larmor frame by

$$\varepsilon \equiv \left(\langle \tilde{x}^2 \rangle \langle \tilde{x}'^2 \rangle - \langle \tilde{x}\tilde{x}' \rangle^2\right)^{1/2} = \left(\langle \tilde{y}^2 \rangle \langle \tilde{y}'^2 \rangle - \langle \tilde{y}\tilde{y}' \rangle^2\right)^{1/2} = \varepsilon_T / 4, \tag{19}$$

where statistical averages are defined in the usual manner by $\langle \cdots \rangle = N^{-1} \int (\cdots) f_b dX dY dP_X dP_Y$. Note that the definition of ε_T in Eq. (19) includes directed transverse motion as well as motion relative to the mean. Defining the *thermal* emittance of the beam by

$$\varepsilon_{th} = 4\left(\beta_b c\right)^{-1}\left[\left\langle x^2\right\rangle\left\langle\left(v_x - V_x\right)^2\right\rangle\right]^{1/2}, \tag{20}$$

it is readily verified that

$$\varepsilon_{th}^2 = \left(1-\omega_b^2\right)\varepsilon_T^2 = \frac{2T_\perp(0,s)r_b^2(s)}{m\gamma_b\beta_b^2c^2}. \tag{21}$$

It follow from Eq. (21) that $\varepsilon_T^2 = \varepsilon_{th}^2 + \omega_b^2\varepsilon_T^2$, where the ω_b^2 term corresponds to the average azimuthal motion in the Larmor frame. Making use of Eqs. (16) and (21), the envelope equation (13) can also be expressed as

$$\frac{d^2}{ds^2}r_b(s) - \frac{\Omega_b(s)}{\beta_b^2c^2}\left[\Omega_b(s)+\Omega_c(s)\right]r_b(s) - \frac{K}{r_b(s)} - \frac{\varepsilon_{th}^2}{r_b^3(s)} = 0, \tag{22}$$

where $\Omega_c(s) = qB_z(s)/\gamma_b mc$ is the relativistic cyclotron frequency including its sign.

The periodically focused rigid-rotor Vlasov equilibrium has two limiting cases which are well known. It recovers the familiar KV beam equilibrium [4-6] by setting the rotation parameter $\omega_b = 0$. It also recovers the familiar constant-radius, uniform-density rigid-rotor Vlasov equilibrium [10] by taking the limit of a uniform magnetic field with $B_z(s) = B_0 =$ const.

We now illustrate with examples of periodically focused rigid-rotor Vlasov equilibria in a periodic solenoidal focusing channel with step-function lattice. Figure 1 shows plots of the normalized axial magnetic field (solid curve), beam radius (dashed curve), and average angular velocity in the laboratory frame (dotted curve) defined in Eq. (16) versus the axial propagation distance s for a rigid-rotor Vlasov equilibrium in a periodic solenoidal focusing channel defined by the ideal periodic step-function

$$\sqrt{\kappa_z(s)} = \begin{cases} \sqrt{\kappa_{z0}} = const., & -\eta/2 \le s/S < \eta/2, \\ 0, & \eta/2 \le s/S < 1-\eta/2. \end{cases} \tag{23}$$

Here, η is the so-called filling factor. In Fig. 1, the beam radius and average angular velocity are determined using Eqs. (13) and (16), respectively, for the choice of system parameters corresponding to: $S\sqrt{\kappa_{z0}} = 3.162$, $\eta = 0.2$, $SK/\mathsf{e}_T = 10$, and $\omega_b = 0.9$; the variables s, $\sqrt{\kappa_z(s)}$, $r_b(s)$, and $\Omega_b(s)$ are scaled by the multipliers S^{-1}, S, $\left(\mathsf{e}_T S\right)^{-1/2}$, and $S/\beta_b c$, respectively. The vacuum and space-charge-depressed phase advances of the

particle betatron oscillations averaged over one lattice period are evaluated to be $\sigma_v = \varepsilon_T \int_0^S ds / r_{b0}^2(s) = 86.6^\circ$ and $\sigma = \varepsilon_T \int_0^S ds / r_b^2(s) = 12.8^\circ$, respectively. Here, $r_{b0}(s) = r_{b0}(s+S)$ is the outer equilibrium beam radius when $K = 0$.

To illustrate the influence of rotation on the periodically focused rigid-rotor Vlasov equilibrium, we plot the relative equilibrium beam radius $r_b(0) / r_b^{KV}(0)$ at $s = 0$ versus the rotation parameter ω_b in Fig. 2, as obtained by solving the envelope equation (22) numerically for the case of the step-function lattice defined in Eq. (23). Here, $r_b^{KV}(0)$ is the outer beam radius for the KV equilibrium $(\omega_b = 0)$ at $s = 0, S, 2S, \cdots$. The choice of system parameters corresponds to: $S\sqrt{\kappa_{z0}} = 3.162$, $\eta = 0.2$, and $SK / \epsilon_{th} = 10$, where ϵ_{th} is the thermal emittance. It is evident in Fig. 2 that the equilibrium beam radius is a minimum when $\omega_b = 0$ (strongest magnetic focusing), and increases rapidly as $|\omega_b| \to 1$. This is because the centrifugal force associated with the beam rotation is defocusing, thereby resulting in a larger beam radius.

Finally, we point out possible applications of the periodically focused rigid-rotor Vlasov equilibrium presented in this article. First, this equilibrium in principle allows for precise matching of an intense beam into a periodic solenoidal focusing channel in terms of detailed phase-space distributions. For example, the value of rotation parameter ω_b can be adjusted experimentally [11] by passing the beam through a step in $B_z(s)$ before the beam enters a periodic solenoidal focusing field. Second, the equilibrium allows for studies of stability properties of a class of intense beams with equilibrium distribution other than the KV distribution.

To summarize, a rigid-rotor Vlasov equilibrium has been obtained for an intense charged-particle beam propagating through a periodic solenoidal focusing field. In the present analysis, the beam has a uniform density profile in the radial direction, and a rigid-rotor angular flow velocity in addition to a constant axial velocity. As special limiting cases, the present analysis includes both the Kapchinskij-Vladimirskij (KV) beam equilibrium (when $\omega_b = 0$) for an intense beam propagating through a periodic solenoidal

focusing field, and the uniform-density, rigid-rotor Vlasov equilibrium for a beam propagating in a uniform magnetic field when $B_z(s) = B_0 = \text{const.}$ The beam envelope equation was derived, and examples of periodically focused rigid-rotor Vlasov beam equilibria were presented. Statistical properties and possible applications of the present equilibrium were also discussed. Study of the stability properties of the present equilibrium is an important area for future investigation.

ACKNOWLEDGMENTS

This research was supported by Department of Energy Grant No. DE-FG02-95ER-40919, Contract No. DE-AC02-76-CHO-3073, and Air Force Office of Scientific Research Grant No. F49620-94-1-0374. The Research by R. Pakter was also supported by CAPES, Brazil.

REFERENCES

1. R. C. Davidson, *Physics of Nonneutral Plasmas* (Addison-Wesley, Reading, Massachusetts, 1990).
2. M. Reiser, *Theory and Design of Charged-Particle Beams* (Wiley & Sons, Inc., New York, 1994).
3. *Space Charge Dominated Beams and Applications of High Brightness Beams*, edited by S. Y. Lee, American Institute of Physics Conference Proceedings **377** (1996).
4. I. M. Kapchinskij and V.V. Vladimirskij, Proceedings of the International Conference on High Energy Accelerators (CERN, Geneva, 1959), p. 274.
5. I. Hofmann, L. J. Laslett, L. Smith, and I. Haber, Particle Accelerators **13**, 145 (1983).
6. C. Chen and R. C. Davidson, Phys. Rev. **E49**, 5679 (1995).
7. R. L. Gluckstern, W.-H. Cheng, and H. Ye, Phys. Rev. Lett. **75**, 2835 (1995).
8. See, for example, Chapters 4 and 9 of Ref. 1.
9. R. C. Davidson and N. A. Krall, Phys. Fluids **13**, 1543 (1970).
10. See p. 99 of Ref. 1.
11. A. J. Theiss, R. A. Mahaffey, and A. W. Trivelpiece, Phys. Rev. Lett. **35**, 1436 (1975).

FIGURE CAPTIONS

Fig. 1 Plots of the normalized axial magnetic field (solid curve), beam radius (dashed curve), and average angular velocity (dotted curve) versus the axial propagation distance s for a periodically focused rigid-rotor Vlasov equilibrium in an applied magnetic field described by the periodic step-function lattice in Eq. (23). Here, the choice of system parameters corresponds to: $S\sqrt{\kappa_{z0}} = 3.162$, $\eta = 0.2$, $SK/\epsilon_T = 10$, and $\omega_b = 0.9$. The variables s, $\sqrt{\kappa_z(s)}$, $r_b(s)$, and $\Omega_b(s)$ are scaled by the multipliers S^{-1}, S, $(\epsilon_T S)^{-1/2}$, and $S/\beta_b c$, respectively.

Fig. 2 Plots of the relative equilibrium beam radius $r_b(0)/r_b^{KV}(0)$ at $s = 0$ versus the rotation parameter ω_b as obtained from Eq. (22) for the step-function lattice defined in Eq. (23). Here, $r_b^{KV}(0)$ is the outer beam radius for the KV equilibrium $(\omega_b = 0)$. The choice of system parameters corresponds to: $S\sqrt{\kappa_{z0}} = 3.162$, $\eta = 0.2$, and $SK/\epsilon_{th} = 10$, where ϵ_{th} is the thermal emittance.

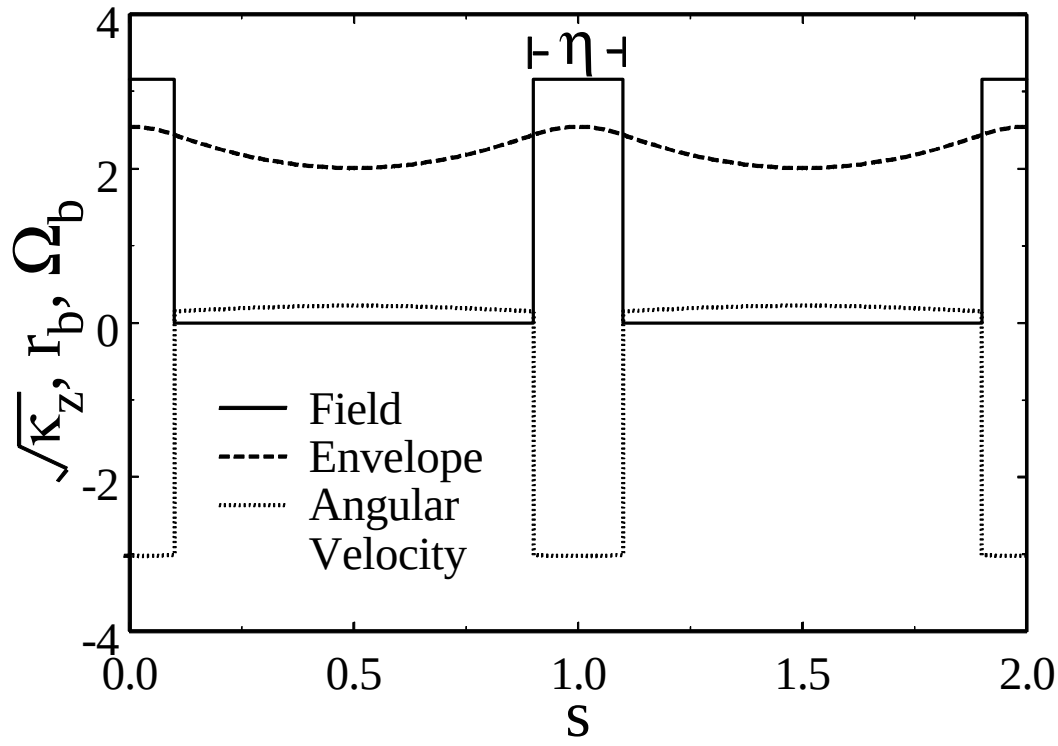

Figure 1
Chen, Phys. Rev. Lett.

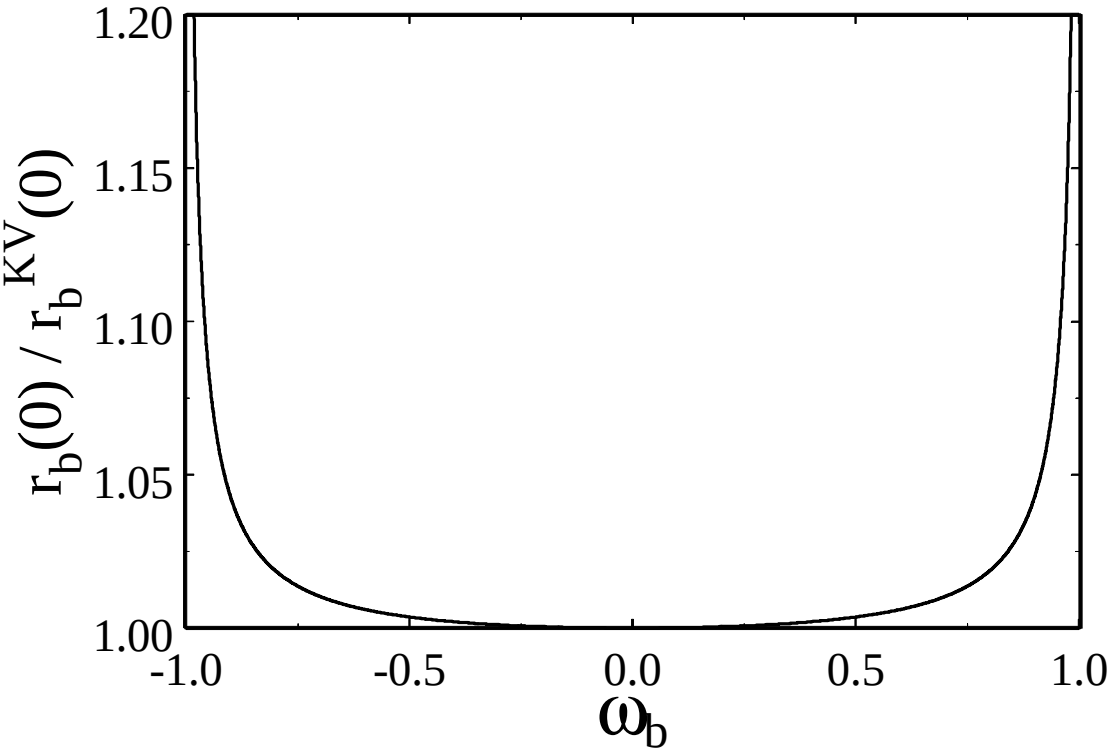

Figure 2
Chen, Phys. Rev. Lett.